ACS APPLIED MATERIALS & INTERFACES

Research Article

www.acsami.org

Layered Double Hydroxides as an Effective Additive in Polymer Gelled Electrolyte based Dye-Sensitized Solar Cells

Hsu-Wen Ho, Wei-Yun Cheng, Yu-Chun Lo, Tzu-Chien Wei, and Shih-Yuan Lu*

Department of Chemical Engineering, National Tsing Hua University, Hsinchu 30013, Taiwan

Supporting Information

ABSTRACT: Layered double hydroxides (LDH), a class of anionic clay materials, were developed as an effective additive for polymer gelled electrolytes for use in dye-sensitized solar cells (DSSC). Carbonate and chloride intercalated Zn-Al LDHs, ZnAl-CO_3 LDH, and ZnAl-Cl LDH were prepared with coprecipitation methods. The addition of the two LDHs significantly improved, in terms of power conversion efficiency (PCE), over the plain poly(vinylidene fluoride-*co*-hexafluoropropylene) (PVDF-HFP) gelled electrolyte and competed favorably with the liquid electrolyte based DSSCs, 8.13% for the liquid electrolyte, 7.48% for the plain PVDF-HFP gelled electrolyte, 8.11% for the ZnAl-CO_3 LDH/PVDF-HFP gelled electrolyte, and 8.00% for the ZnAl-Cl LDH/PVDF-HFP gelled electrolyte based DSSCs. The good performance in PCEs achieved by the LDH-loaded DSSCs came mainly from the significant boost in open circuit voltages (V_{oc}), from 0.74 V for both the liquid electrolyte and PVDF-HFP gelled electrolyte based DSSCs to 0.79 V for both the ZnAl-CO_3 LDH/PVDF-HFP and ZnAl-Cl LDH/PVDF-HFP gelled electrolyte based DSSCs. The boost in V_{oc} was contributed mainly by the positive shift in redox potential of the redox couple, I^-/I_3^-, as revealed from cyclic voltammetry analyses. As for the long-term stability, PCE retention rates of 96 and 99% after 504 h were achieved by the ZnAl-CO_3 LDH/PVDF-HFP and ZnAl-Cl LDH/PVDF-HFP gelled electrolyte based DSSCs, respectively, appreciably better than 92% achieved by the liquid electrolyte based one after 480 h.

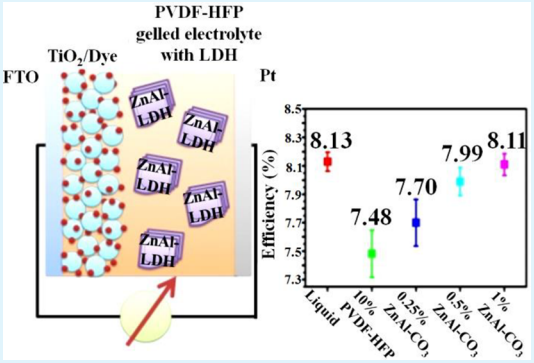

KEYWORDS: *layered double hydroxide, dye-sensitized solar cell, polymer gelled electrolytes, electrolyte additive*

1. INTRODUCTION

Dye-sensitized solar cells (DSSC) continue to draw a great deal of research attention as a promising alternative clean energy device because of the simplicity and low cost involved in the manufacturing process and the reasonable power conversion efficiency (PCE) achieved. The boost in PCE to a record high of 13% reported by Mathew et al.[1] in 2014 makes DSSCs even more competitive. One of the key issues yet to be fully resolved is the volatility, leakage, and poor long-term stability associated with the use of liquid electrolytes in DSSCs. Intensive and extensive research efforts have been devoted to the development of gel or solid electrolytes to tackle the issue. One of the key issues for the development of gel or solid electrolytes is to lessen the drop in the power conversion efficiency caused by the reduced ionic mobility in gel or solid electrolytes.

For solid electrolytes, the poor electrode contact and pore-filling ability at the electrolyte/electrode interface often hampers the boost in PCE.[2−5] Even if high PCEs can sometimes be achieved, the reliability and consistency of the cell performance are of great concern. Gel electrolytes, on the other hand, possess the advantages of low volatility and superior long-term stability as compared with liquid electrolytes, and of good electrolyte/electrode contacts as compared with solid electrolytes.[2,6−20] In the past few years, use of polymer gelled electrolytes containing performance boosting additives has been a promising approach.[6−8,16−20] Particularly, clay materials, because of their high chemical stability, ion exchange ability, and natural abundance, have been a popular candidate as the additive.[2] Tu et al. composited exfoliated montmorillonite with poly(*n*-isopropylacrylamide) (PNIPAAm) to gel the electrolyte. The inclusion of the exfoliated montmorillonite reduced the charge transport/transfer impedances of the cell, leading to a PCE improvement from 3.17 to 5.4% as compared with the plain PNIPAAm gelled electrolyte based DSSC.[6] Geng et al. found that addition of montmorillonite to poly(ethylene oxide) (PEO) gelled electrolytes can efficiently retard the charge recombination that occurs at the TiO_2/dye/electrolyte interfaces.[7] Lai et al. used poly(vinylidene fluoride-*co*-hexafluoropropylene) (PVDF-HFP) gelled electrolytes with mica nanoparticles as the additive to reduce the crystallinity of the polymer, leading to a higher PCE from 3.5 to 5.7% at a mica loading of 3 wt %.[8]

In addition to clay materials, carbonaceous materials, including graphene, graphene oxide, graphite, and multiwalled carbon nanotubes, conducting polymers, such as polyaniline and polypyrrole, and mesoporous silica nanoparticles have also

Received: May 6, 2014
Accepted: September 23, 2014
Published: September 23, 2014

been tested as effective additives for gel electrolyte DSSCs.[16−20] Yuan et al. developed a freeze-dried microporous polyacrylate−poly(ethylene glycol) (PAA-PEG) matrix to host conducting graphene, graphene oxide, and graphite to enhance the loading and ionic conductivity of the electrolyte. The DSSCs fabricated using the PAA-PEG/graphene, PAA-PEG/graphene oxide, and PAA-PEG/graphite composites as the gel electrolyte showed PCEs of 7.74, 6.49, and 5.63%, respectively, significantly higher than 5.02% obtained by a plain PAA-PEG based DSSC.[16] The same idea was also applied to conducting polymer systems, including polyaniline and polypyrrole, by Yuan et al. The PCE increased from 5.02% of the plain PAA-PEG based DSSC to 7.12 and 6.53% of the PAA-PEG/PANi and PAA-PEG/PPy based DSSCs, respectively.[18] Neo et al. used multiwalled carbon nanotubes to reinforce the network strength and shorten the ionic diffusion length of graphene oxide gelled electrolytes, and achieved a PCE boost from 6.54 to 7.12%.[17] Chen et al. used mesoporous silica nanoparticles (MSN) to enhance the light harvesting and ion diffusion of the gel electrolyte. An increase of the PCE from 4.62% of the plain gel electrolyte based DSSC to 5.45% of the MSN-incorporated gel electrolyte based DSSC was acquired.[19] Yuan et al. incorporated graphene, graphene oxide, and nanographite to a microporous poly(acrylic acid)−cetyltrimethylammonium bromide (PAA-CTAB) matrix to form conducting gel electrolytes. The PCE was increased from 6.07% of the plain PAA-CTAB based DSSC to 7.06, 6.35, and 6.17% of the graphene, graphene oxide, and nanographite incorporated PAA-CTAB based DSSCs, respectively.[20]

Among the above-mentioned additive materials, montmorillonite and mica belong to the class of cationic clays, carrying negative charges on their hydroxide layers counterbalanced by positive interlayer ions. The popular electrolyte redox couple for DSSCs, I^-/I_3^-, however, contains anions. The use of anionic clay materials, containing interlayer anions, together with their high chemical stability, ion exchange ability, and natural abundance, may prove advantageous for DSSCs because of the anion-exchange ability of the material.[2]

In this work, layered double hydroxides (LDH), a class of anionic clay materials, were developed as the additive for PVDF-HFP gelled electrolytes. PVDF-HFP is photochemically stable and contains fluoride ions of strong electronegativity that can coordinate well with Li^+ to increase the solubility of LiI in the electrolyte, and is thus a suitable and popular polymer for electrolyte gelling purposes. Carbonate and chloride intercalated Zn-Al LDHs, ZnAl-CO_3 LDH, and ZnAl-Cl LDH were prepared with coprecipitation methods to serve as the additive for the polymer gelled electrolyte. The interlayer anions interact with the hydroxide layer through electrostatic forces and hydrogen bonds, and exhibit different affinity with the hydroxide layer and thus different ion exchange ability. The affinity of the relevant ions of the present study is in the order of carbonate > chloride > iodide.[21] One thus expects to observe some extent of anion exchange of the two LDHs when in use as the electrolyte additive. It is also interesting to investigate if the ion affinity significantly affects the DSSC performance.

It was found that the addition of the two LDHs, in terms of PCEs, significantly improved over the plain PVDF-HFP gelled electrolyte and competed favorably with the liquid electrolyte based DSSCs. The PCE of the gel electrolyte based DSSC was increased from 7.48% to 8.11% of the 1 wt % ZnAl-CO_3 LDH enhanced gel electrolyte based DSSC. The good performance in PCE achieved by the LDH-loaded DSSCs was mainly contributed by the significant boost in open circuit voltages (V_{oc}), which was further found to come from the positive shift in the redox potential of the redox couple, I^-/I_3^-, as revealed by cyclic voltammetry analyses. As for the long-term stability, PCE retention rates of 96 and 99% after 504 h were achieved for the ZnAl-CO_3 LDH/PVDF-HFP and ZnAl-Cl LDH/PVDF-HFP gelled electrolyte based DSSCs, respectively, appreciably better than 92% achieved by the liquid electrolyte based one after 480 h. Anionic LDHs were thus proved to be a promising performance boosting additive for polymer gelled electrolyte based DSSCs.

2. EXPERIMENTAL SECTION

2.1. Preparation of ZnAl-CO3 LDH and ZnAl-Cl LDH. ZnAl-CO_3 LDH was prepared with a coprecipitation method.[22] Briefly, an aqueous solution of 0.4 M $Zn(NO_3)_2{\cdot}6H_2O$ (99%, Showa) and 0.2 M $Al(NO_3)_3{\cdot}9H_2O$ (>95%, Showa) was mixed with an aqueous solution of 0.3 M Na_2CO_3 (99.5%, Showa) and 1.5 M NaOH (99.5%, Showa). The amount of the latter aqueous solution was controlled to achieve a pH value of 10 for the final mixed solution. The mixed solution was left undisturbed for 24 h. The resulting precipitates were rinsed with deionized (DI) water, followed by drying at 60 °C for 24 h to afford the ZnAl-CO_3 LDH. ZnAl-Cl LDH was prepared with a coprecipitation method.[23] An aqueous solution of 200 mL containing 0.75 M $ZnCl_2$ (95%, Showa) and 0.25 M $AlCl_3$ (98.5%, Showa) and the other aqueous solution of 200 mL containing 1 M NaCl and 1 M NaOH were added into 100 mL of DI water at an addition rate of 50 mL/h at 80 °C under vigorous stirring. All solutions were purged with nitrogen before mixing. A suitable amount of 2 M NaOH was added to the resulting solution to achieve a solution pH value of 10. The final mixed solution was further stirred at 90 °C for 24 h. The resulting precipitates were rinsed with DI water, followed by drying at 60 °C for 24 h to afford the ZnAl-Cl LDH.

2.2. Preparation of Electrolyte Immersed LDHs. LiI (99.9%, Aldrich), I_2 (99.5%, Fluka), and $LiClO_4$ (>95%, Aldrich) of 50, 10, and 500 mM, respectively, were dissolved in 2 mL of acetonitrile (99.8%, JT Baker) in a drybox. An amount of 1 wt % LDH, ZnAl-CO_3, or ZnAl-Cl was immersed in the above solution at 70 °C for 2 h under stirring. The treated LDH was then rinsed thoroughly with DI water before drying at 60 °C overnight to afford the electrolyte immersed LDH.

2.3. Preparation of Liquid Electrolyte and Polymer Gelled Electrolytes. The liquid electrolyte was prepared by dissolving 0.1 M LiI, 0.6 M 1-propyl-2,3-dimethylimidazolium iodide (DMPII, 99%, Aldrich), 0.05 M I_2, and 0.5 M 4-*tert*-butylpyridine (TBP, 98%, Fluka) into acetonitrile in a drybox. The plain polymer gelled electrolyte was prepared by first dispersing 10 wt % PVDF-HFP (Mw = 400 000, Aldrich) in 0.5 mL of liquid electrolyte at 70 °C under stirring for 2 h and then cooled in a 5 °C environment to gel to afford the product. As for the LDH-loaded polymer gelled electrolytes, the procedures were the same except that a desired amount of LDH was added together with the 10 wt % PVDF-HFP.

2.4. Assembly of DSSCs. TiO_2 paste was screen-printed onto a fluorine doped tin oxide (FTO) glass (Nippon Sheet Glass Co., 3.1 mm, <30 Ω/cm^2) of 0.4 × 0.4 cm to form the photoanode layer. The Pt based counter electrodes were prepared by sputtering deposition of a 50 nm thick Pt film onto a silicon wafer. The photoanodes with a working area of 0.16 cm^2 were heated at 120 °C for 5 min to remove the trapped air and moisture. They were then soaked in a 0.3 mM *cis*-bis(isothiocyanato)bis(2,2′-biprydi-4,4′-dicarboxylatoruthenium(II)-bis-tetrabutylammonium (N719, Solaronix) solution for 12 h for dye adsorption. Here, the solvent for the N719 dye was composed of *t*-butanol (99.5%, Reidel-de Haen) and acetonitrile at a volumetric ratio of 1:1. To assemble the cell, a spacer with a thickness of 60 μm was used to connect the counter electrode and photoanode.

2.5. Characterizations. The thickness of the photoanode was determined with a surface texture and contour measuring instrument (Surfcom Flex, Accretech). An X-ray diffractometer (UltimaIV,

Rigaku) was used to determine the crystalline structure of the product LDHs. The functional groups of the LDH samples were analyzed with a Fourier transform infrared spectrometer (Spectrum RX-I, PerkinElmer). The iodide content of the electrolyte immersed LDHs were characterized with high resolution X-ray photoelectron spectrometry (XPS, PHI Quantera SXM, ULVAC-PHI). Field-emission scanning electron microscopy (FESEM, S-4700, Hitachi) was used to observe the morphology of the LDHs. The current density−voltage (J−V) curves of the cells were recorded with a source meter (Kiethley 236, Kiethley) under illumination of a solar simulator (Yamashita Denso,YSS-E40; AM 1.5, 100 mW cm^{-2}) calibrated by a reference Si solar cell (SN2008-152, Yamashita). The redox potential of the electrolyte was determined as the arithmetic average of the reduction peak and oxidation peak potentials of the electrolyte as recorded in the cyclic voltammogram. The base electrolyte was composed of 50 mM LiI, 500 mM $LiClO_4$, and 10 mM I_2 dissolved in acetonitrile. For the PVDF-HFP gelled electrolyte, 10 wt % PVDF-HFP was added into the base electrolyte. As for the LDH-loaded PVDF-HFP gelled electrolytes, 1 wt % of ZnAl-CO_3 LDH or ZnAl-Cl LDH was further added. Before the cyclic voltammetry (CV) recording, the gelled electrolytes were heated to melt. Pt sputtered silicon wafers served as the counter and working electrodes, and Ag/$AgNO_3$(0.01 M in acetonitrile, 0.54 V vs standard hydrogen electrode) as the reference electrode. The CV was recorded at a scan rate of 20 mV/s. Electrochemical impedance spectroscopy was conducted in dark with a potentiostat (PGSTAT30, AUTOLAB). For the long-term stability test, the assembled cells were measured for the J−V curves at selected times and stored in dark when not under measurement.

3. RESULTS AND DISCUSSION

Figure 1(a) shows the XRD patterns of the ZnAl-CO_3 and ZnAl-Cl LDHs. The patterns agree very well with those reported previously in the literature.[22,24−26] The sharp and well-defined diffraction peaks of the patterns indicate good crystallinity of the product, and the sharp diffraction peak of the basal plane, (003), located at the low angle region is a pronounced characteristics of the layered structure.[27] If examined closely, one observes a slight left shift of the diffraction peaks for the ZnAl-Cl LDH as compared with those of the ZnAl-CO_3 LDH. The slight left shift corresponds to an enlargement of the interlayer distance from 0.77 nm for the ZnAl-CO_3 LDH to 0.798 nm for the ZnAl-Cl LDH. This phenomenon is in good agreement with that observed in previous literature,[25,26] and is caused by the slightly larger size of chloride. Figure 1b shows the product morphologies of the ZnAl-CO_3 (left panel) and ZnAl-Cl (right panel) LDHs. Both LDHs appear as thin sheets of sizes of 100−200 nm, further signifying their layered structure characteristics.

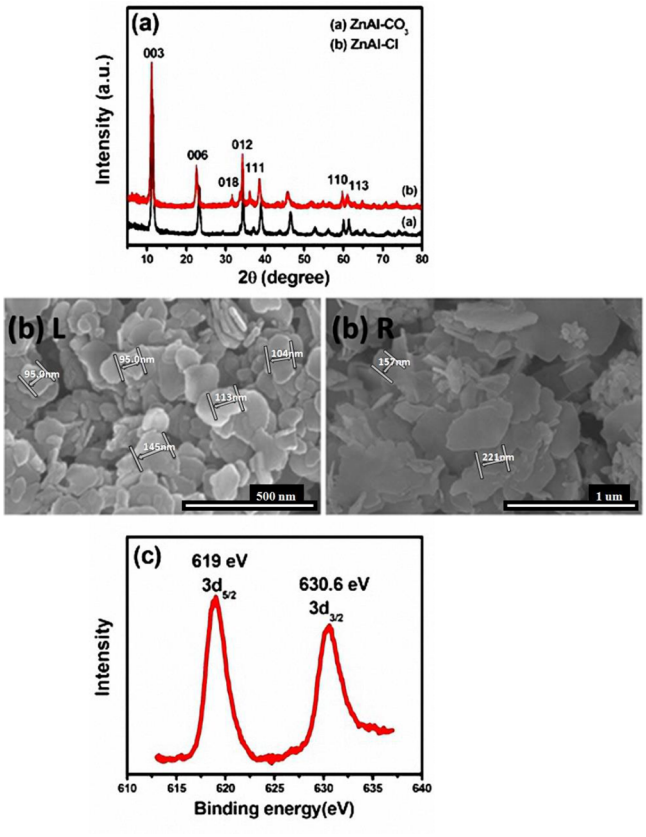

Figure 1. (a) XRD patterns of ZnAl-CO_3 and ZnAl-Cl LDHs. (b) SEM images of ZnAl-CO_3 (left) and ZnAl-Cl (right) LDHs. (c) XPS of iodide solution immersed ZnAl-CO_3 LDH.

The characteristic functional groups contained in the two LDHs were identified with Fourier transform infrared spectroscopy (FTIR) and shown in Figure S1 (Supporting Information). The pronounced broad band located at 3458 cm^{-1} was contributed by the O−H vibration of the −OH groups contained in the adsorbed interlayer water and the hydroxide layer.[27,28] The band located at 1636 cm^{-1} was caused by the bending vibration of δ HOH of the adsorbed interlayer water.[28] The one at 1362 cm^{-1} was contributed by the $\nu 3$ stretching mode of the carbonate.[27] This band was much stronger for the ZnAl-CO_3 LDH than for the ZnAl-Cl LDH, as it should. The minor amount of carbonate found in the ZnAl-Cl LDH may come from the absorption of atmospheric CO_2. The band at 667 cm^{-1} was generated by the M−O or O−M−O (M = Zn, Al) vibrations.[28]

To investigate the iodide exchange ability of the two LDHs, we immersed the LDHs in iodide containing solutions at 70 °C for 2 h and examined the morphology, crystalline structure, and composition of the LDHs after the immersion. The morphology (Figure S2, Supporting Information) and crystalline structure (Figure S3, Supporting Information) of the immersed LDHs remained almost unchanged, only that the diffraction patterns became less well-defined, implying a slightly deteriorated layered structure, possibly caused by the disordered placement of a minor amount of iodide within the interlayer. No appreciable left shifts in the main diffraction peak position were observed because the concentration of the iodide was only minor in the interlayer. The concentrations of iodide in the immersed LDHs were determined by EDX analyses and were 0.33 at. % for the ZnAl-CO_3 LDH and 0.65 at. % for the ZnAl-Cl LDH. This trend is consistent with the affinity order of carbonate versus chloride. Chloride has weaker affinity toward the hydroxide layer and is thus easier to be displaced by iodide.[21]

The presence of iodide after the immersion was further confirmed with XPS measurements. Figure 1c shows the XPS of the immersed ZnAl-CO_3 LDH, which displays characteristic binding energies of iodide at 618.9 ($3d_{5/2}$) and 631 ($3d_{3/2}$) eV, in good agreement with those reported in the literature.[2,29]

The performances of DSSCs assembled using the present LDH-loaded PVDF-HFP gelled electrolytes were compared with those achieved by DSSCs using liquid electrolyte and plain PVDF-HFP gelled electrolyte. The mass loading of the LDH was varied from 0.25 to 1 wt % to investigate its effects on the performances of the corresponding DSSCs. Figure 2 shows the resulting J−V curves. As compared with the liquid electrolyte case, both LDH cases produced higher open-circuit voltages

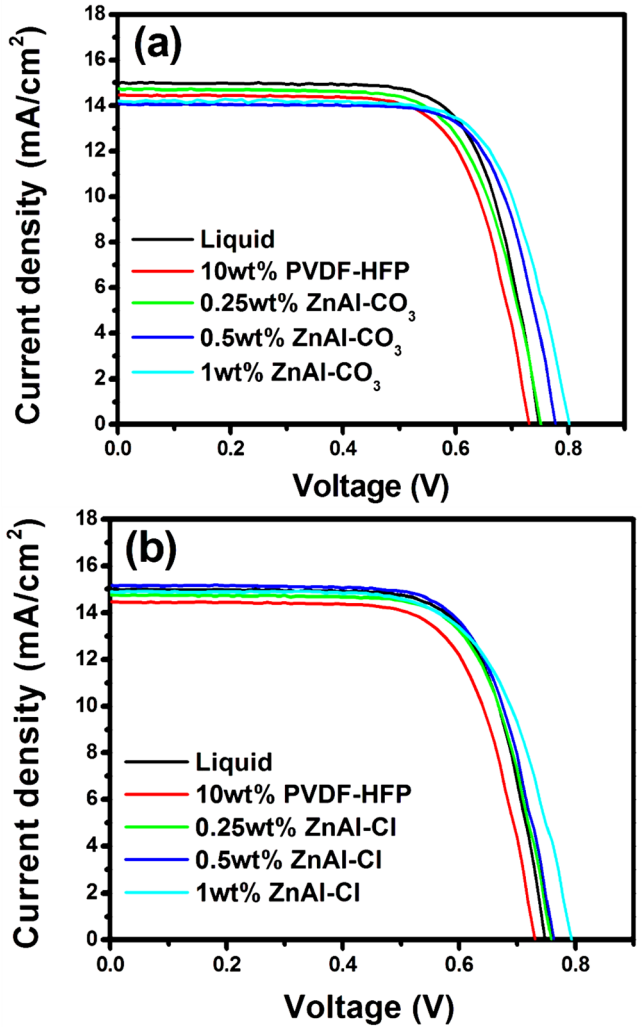

Figure 2. Photocurrent density–voltage (J–V) plots of liquid electrolyte, plain PVDF-HFP gelled electrolyte, (a) ZnAl-CO_3 LDH/PVDF-HFP gelled electrolyte, and (b) ZnAl-Cl LDH/PVDF-HFP gelled electrolyte based DSSCs.

but slightly lower short circuit current density (J_{sc}). On the other hand, the plain PVDF-HFP case achieved generally lower V_{oc} and J_{sc} than those of LDH-loaded cases. Because the power conversion efficiency (PCE = $V_{oc} \times J_{sc} \times FF/P_{in}$, FF = fill factor, P_{in} = power of incident light) is directly proportional to V_{oc} and J_{sc}, one thus expects that the addition of LDH improves over the plain PVDF-HFP case in power conversion efficiency.

Figures 3 and 4 show the four essential performance parameters derived from the J–V curves, PCE, V_{oc}, J_{sc}, and FF, for the two LDH-loaded cases as functions of LDH mass loading. Also included for comparison are data collected from the liquid electrolyte case. As expected, the addition of LDH improved over the plain PVDF-HFP case in PCE. The PCEs of the two LDH-loaded cases are comparable to those of the liquid electrolyte case. Generally speaking, as compared with the corresponding data of the liquid electrolyte case, the LDH addition boosted the V_{oc}, accompanied by slight reduction in J_{sc} and relatively unchanged FF. The end result was that the improvement in V_{oc} compensated the loss in J_{sc}, leading to comparable PCEs with those of the liquid electrolyte case. As for the plain PVDF-HFP case, the improvement in PCE achieved by the LDH addition mainly came from the increase in V_{oc}. The J_{sc} was not influenced by the loading of LDH. Figure S4 (Supporting Information) shows the incident photo-to-current conversion efficiency (IPCE) spectra of the plain PVDF-HFP and LDH-loaded cases and no appreciable differences can be observed, in agreement with the J_{sc} results. The boost in V_{oc} increased with increasing LDH loading. The type of LDH, carbonate or chloride intercalated, however did not result in significant differences in cell performance.

To further understand the effects of LDH addition on the cell performance, we conducted electrochemical impedance spectroscopy (EIS) in the dark to study the resistance associated with the electron transport across the photoanode layer, R_t, and the resistance associated with the electron transfer of charge recombination occurring at the photoanode/electrolyte interface, R_{ct}. The photoinduced electrons, injected from the excited dye molecule into the photoanode domain, need to be transported across the photoanode layer to reach the current collector. These electrons may also recombine with the oxidized dye molecules or I_3^- and get lost before reaching the current collector. To increase the PCE, the resistance to the electron transport, R_t, should be small, whereas the resistance to the charge transfer, R_{ct}, should be large. The EIS was conducted in the dark to avoid the interference coming from the photon-induced charge transport. The applied potential was first chosen to be in the range of 0.6–0.7 V according to the system responses revealed by the corresponding Nyquist plots. In the potential range of 0.6–0.7 V, the Nyquist plot displayed the most distinct contributions of both R_t and R_{ct}, from which the behavior of both resistances can be better explored (Figure S5, Supporting Information).

Figure 5 shows R_t and R_{ct}, as determined from the fitting of the impedance data using the transmission line model,[30] as functions of applied potential for the two LDH-loaded cases. Both R_t and R_{ct} decreased logarithmically with increasing applied potential and increased with increasing LDH loading. The effects induced by the LDH addition can be attributed to the reduced adsorption amount of Li^+ on the surface of the photoanode, because of the competition for Li^+ coming from the LDH. Part of the lithium ion present in the electrolyte was adsorbed onto the surface of the photoanode, causing a positive shift of the conduction band of the photoanode.[29,31] When the LDH was added, the anions of the LDH competed with the TiO_2 of the photoanode for Li^+ adsorption, thus reducing the amount of Li^+ adsorption on the photoanode surface and thus less positive shift in its conduction band. The end result was a negative shift in the conduction band of the TiO_2 electrode, taking the PVDF-HFP case as a comparison base. This negative shift in the conduction band made it more difficult for electron injection, thus reduced electron densities in the photoanode and higher R_t and R_{ct}.[32] The negative shift in the conduction band of the TiO_2 electrode can be confirmed with the chemical capacitance data derived from the EIS analysis. Figure S6 (Supporting Information) shows the chemical capacitance versus potential plot for both LDH cases. When the conduction band of the TiO_2 electrode shifts to the more negative region, the electron density at the TiO_2 electrode deceases, leading to lower chemical capacitances. As evident from Figure S5 (Supporting Information), for both LDH cases, the chemical capacitance dropped with increasing LDH loading.

The negative shift in the conduction band helped boosting the V_{oc} of the cell, because V_{oc} is basically the potential difference between the conduction band of the photoanode and the redox potential of the electrolyte couple, I^-/I_3^-. Although

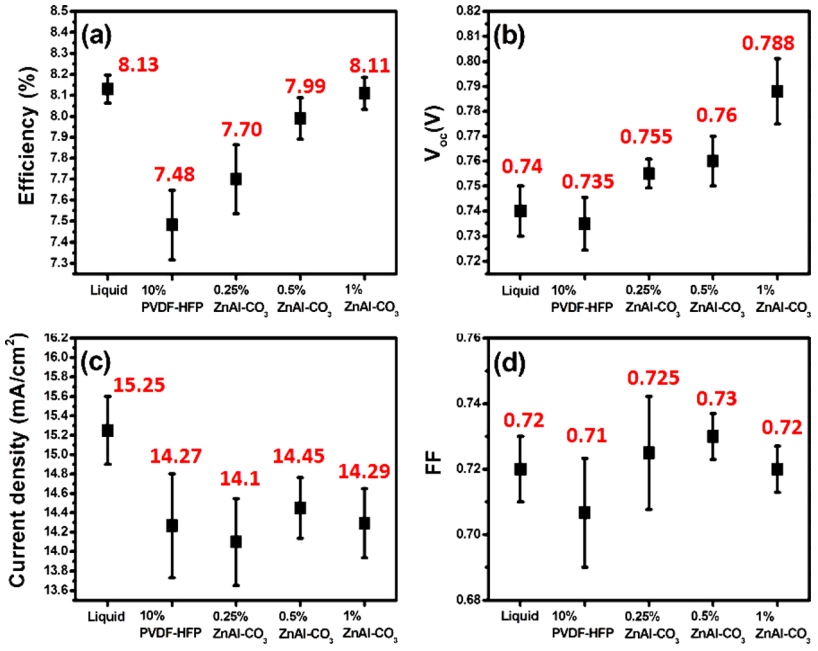

Figure 3. (a) PCE, (b) V_{oc}, (c) J_{sc}, and (d) FF of liquid electrolyte, plain PVDF-HFP gelled electrolyte, and ZnAl-CO_3 LDH/PVDF-HFP gelled electrolyte based DSSCs.

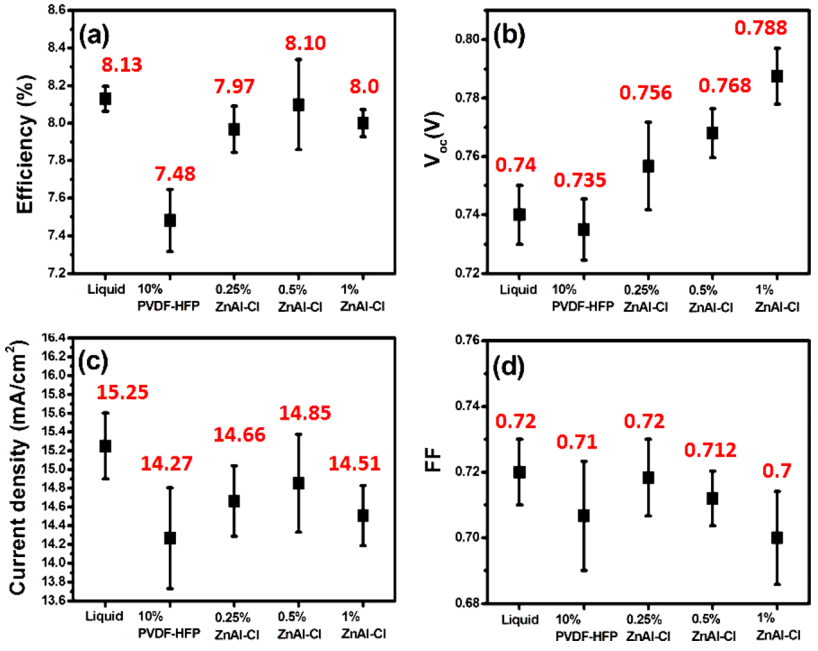

Figure 4. (a) PCE, (b) V_{oc}, (c) J_{sc}, and (d) FF of liquid electrolyte, plain PVDF-HFP gelled electrolyte, and ZnAl-Cl LDH/PVDF-HFP gelled electrolyte based DSSCs.

the electron density was reduced when the negative conduction band shift occurred, the recombination loss of the electron was also reduced because of the higher R_{ct}. The two competing effects somewhat balanced, leading to relatively unchanged J_{sc}, as shown in Figures 3 and 4. If examined closely, for both LDH cases, the values of R_{ct} were about 1 order of magnitude larger than those of the corresponding R_t. This means that most of the electrons injected into the TiO_2 electrode has the chance to be transported across the TiO_2 layer to reach the current collector, instead of being recombined with I_3^- or oxidized dye molecules and lost. It is an essential characteristic for high efficiency DSSCs.

As revealed in Figures 3 and 4, the improvement in PCE for LDH-loaded cases came mainly from the boost in V_{oc}. Part of the V_{oc} boost came from the reduced Li^+ adsorption on the TiO_2 surface. We further examined the redox potential of the electrolytes to investigate other possible contributions to the V_{oc} boost. Figure 6 shows the cyclic voltammograms recorded for four different electrolytes, liquid, plain PVDF-HFP, ZnAl-CO_3 LDH loaded, and ZnAl-Cl LDH loaded. There appeared two sets of redox pairs, the first pair located in the high potential region came from the redox reaction of $2I_2 + 2e^- \leftrightarrow 2I_3^-$ and the second pair was contributed by $I_3^- + 2e^- \leftrightarrow 3I^-$, which was the one occurring at the electrolyte/counter

dx.doi.org/10.1021/am504912d | ACS Appl. Mater. Interfaces 2014, 6, 17518−17525

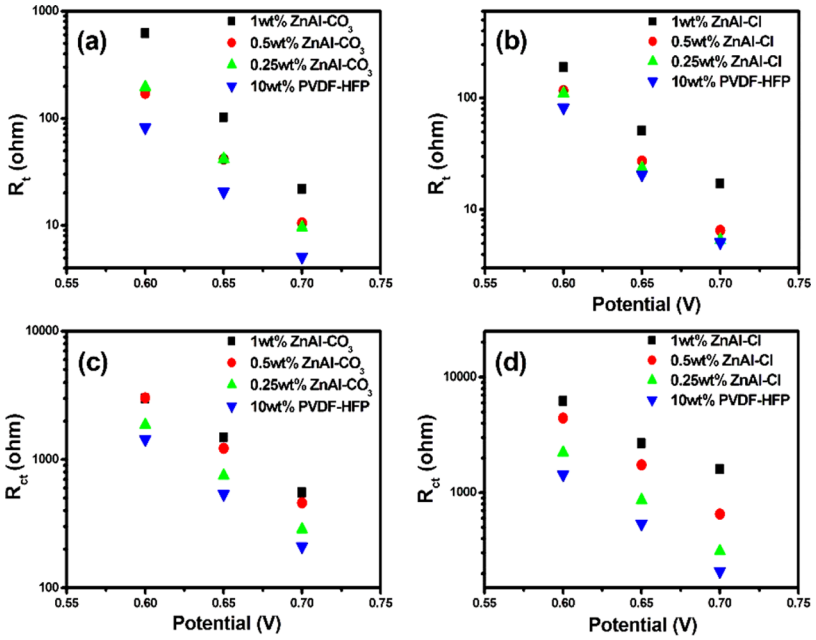

Figure 5. (a) R_t and (c) R_{ct} for ZnAl-CO_3 LDH/PVDF-HFP gelled electrolyte based DSSCs as functions of ZnAl-CO_3 LDH loading. (b) R_t and (d) R_{ct} for ZnAl-Cl LDH-loaded case.

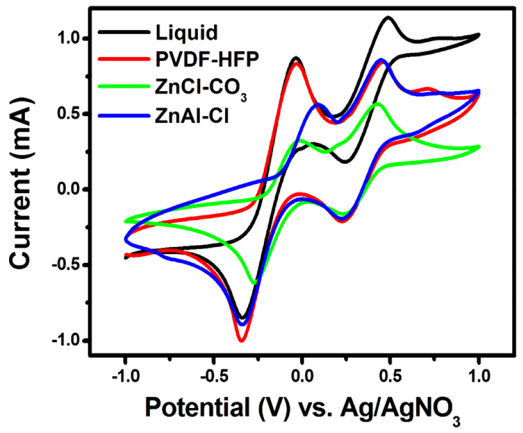

Figure 6. Cyclic voltammograms recorded for four different electrolytes: liquid, plain PVDF-HFP gelled, ZnAl-CO_3 LDH/PVDF-HFP gelled, and ZnAl-Cl LDH/PVDF-HFP gelled.

electrode interface for I^- regeneration.[33] We focus on the second pair for its relevancy to the cell performance. The redox potential was determined as the arithmetic average of the reduction and oxidation peak potentials. For the liquid electrolyte case, the value was 0.356 V versus normal hydrogen electrode (NHE), in good agreement with that reported in literature.[34] As for the plain PVDF-HFP case, it was 0.35 V, close to that of the liquid electrolyte case. This indicated that the gelation of the liquid electrolyte with PVDF-HFP did not affect the redox potential of the I^-/I_3^- couple. The addition of LDHs, however, produced positive shifts for the redox potential, 0.05 V for the ZnAl-CO_3 case and 0.07 V for the ZnAl-Cl case. These positive shifts in redox potential contributed significantly to the V_{oc} boost of the cell. The mechanism for the positive shift of redox potential upon addition of the LDH is not yet understood, but is conjectured to be related to the ion exchange ability of the LDH. The redox potential (E_{redox}) of the electrolyte is given by the Nernst equation as[34]

$$E_{redox} = E^0 + \frac{RT}{2F}\ln\frac{[I_3^-]}{[I^-]^3}$$

where E^0 is the formal potential, R the gas constant, T the absolute temperature, and F the Faraday constant. When the LDH is added to the electrolyte, part of the iodide is ion-exchanged to the interlayer of the LDH as discussed in the earlier section. This would reduce the concentration of iodide in the electrolyte and increase E_{redox} according to the above equation, leading to the V_{oc} boost. The positive shift in E_{redox} increases with increasing LDH loading and gives rise to increasing V_{oc}, in good agreement with the trend revealed by Figures 3b and 4b for V_{oc}.

The long-term stability of the cells assembled by using the LDH-loaded PVDF-HFP gelled electrolytes was tested against that of the liquid electrolyte based cells. The PCE retention rate of the liquid electrolyte case after 480 h was 92%, while those of the LDH-loaded cases were 96% for the ZnAl-CO_3 LDH case and 99% for the ZnAl-Cl LDH case after 504 h. The normalized PCE versus time plot for the three cases is shown in Figure S7 (Supporting Information). It is evident from Figure S7 (Supporting Information) that the LDH-loaded PVDF-HFP gelled electrolyte based DSCs outperformed the liquid electrolyte based one, in terms of long-term stability. The curves for the two LDH cases fluctuated, but remained in the high retention rate region, whereas that of the liquid electrolyte based cell dropped monotonically. The comparison of the three curves showed the superior long-term stability of the LDH based cells.

4. CONCLUSIONS

Layered double hydroxides, a kind of anionic clay materials, were developed as an effective additive for polymer gelled electrolytes. Two kinds of ZnAl LDH were tested, one with carbonate and the other chloride as the interlayer anion. The

addition of both LDHs significantly boosted the V_{oc} of the cell and improved over the plain PVDF-HFP based cell in PCE. The V_{oc} boost was found to mainly come from the positive shift of the redox potential of the electrolyte. The two LDH-loaded cases exhibited comparable PCE as that of the liquid electrolyte case, but outperformed the liquid electrolyte case in terms of long-term stability. The present LDH-loaded, polymer gelled electrolytes thus are a promising alternative to the traditional liquid electrolyte for DSSC applications.

■ ASSOCIATED CONTENT

Supporting Information

FTIR spectra for ZnAl-CO_3 LDH and ZnAl-Cl LDH, SEM images and XRD patterns for electrolyte immersed ZnAl-CO_3 LDH and ZnAl-Cl LDH, IPCE spectra for plain PVDF-HFP, ZnAl-CO_3 LDH/PVDF-HFP and ZnAl-Cl LDH/PVDF-HFP gelled electrolyte based DSSCs, Nyquist plot for ZnAl-Cl LDH/PVDF-HFP gelled electrolyte based DSSC at 0.6 V, chemical capacitance versus potential plots for ZnAl-CO_3 LDH/PVDF-HFP and ZnAl-Cl LDH/PVDF-HFP gelled electrolyte based DSSCs, and normalized PCE versus time plot for liquid electrolyte, ZnAl-CO_3 LDH/PVDF-HFP and ZnAl-Cl LDH/PVDF-HFP gelled electrolyte based DSSCs. This material is available free of charge via the Internet at http://pubs.acs.org.

■ AUTHOR INFORMATION

Corresponding Author

*S.-Y. Lu. E-mail: SYLu@mx.nthu.edu.tw.

Notes

The authors declare no competing financial interest.

■ ACKNOWLEDGMENTS

This work is financially supported by the National Science Council of the Republic of China (Taiwan) under grant NSC-101-2221-E-007-111-MY3 and by the Low Carbon Energy Research Centre of the National Tsing-Hua University. The authors thank Dr. Kuan-Ting Lee and Mr. Peng-Kai Hong of the Department of Chemical Engineering of the National Tsing Hua University, Hsinchu, Taiwan for the assistance in processing experimental data.

■ REFERENCES

(1) Mathew, S.; Yella, A.; Gao, P.; Humphry-Baker, R.; Curchod, B. F. E.; Ashari-Astani, N.; Tavernelli, I.; Rothlisberger, U.; Nazeeruddin, K.; Grätzel, M. Dye-Sensitized Solar Cells with 13% Efficiency Achieved through the Molecular Engineering of Porphyrin Sensitizers. *Nat. Chem.* **2014**, *6*, 242−247.

(2) Wang, X.; Kulkarni, S. A.; Ito, B. I.; Batabyal, S. K.; Nonomura, K.; Wong, C. C.; Gratzel, M.; Mhaisalkar, S. G.; Uchida, S. Nanoclay Gelation Approach toward Improved Dye-Sensitized Solar Cell Efficiencies: An Investigation of Charge Transport and Shift in the TiO_2 Conduction Band. *ACS Appl. Mater. Interfaces* **2013**, *5*, 444−450.

(3) Wang, P.; Zakeeruddin, S. M.; Moser, J. E.; Nazeeruddin, M. K.; Sekiguchi, T.; Gratzel, M. A Stable Quasi-Solid-State Dye-Sensitized Solar Cell with an Amphiphilic Ruthenium Sensitizer and Polymer Gel Electrolyte. *Nat. Mater.* **2003**, *2*, 402−407.

(4) Stergiopoulos, T.; Arabatzis, I. M.; Katsaros, G.; Falaras, P. Binary Polyethylene Oxide/Titania Solid-State Redox Electrolyte for Highly Efficient Nanocrystalline TiO_2 Photoelectrochemical Cells. *Nano Lett.* **2002**, *2*, 1259−1261.

(5) Gui, E. L.; Kang, A. M.; Pramana, S. S.; Yantara, N.; Mathews, N.; Mhaisalkar, S. G. Effect of TiO_2 Mesoporous Layer and Surface Treatments in Determining Efficiencies in Antimony Sulfide-(Sb_2S_3) Sensitized Solar Cells. *J. Electrochem. Soc.* **2012**, *159*, B247−B250.

(6) Tu, C.-W.; Liu, K.-Y.; Chien, A.-T.; Yen, M.-H.; Weng, T.-H.; Ho, K.-C.; Lin, K.-F. Enhancement of Photocurrent of Polymer-Gelled Dye-Sensitized Solar Cell by Incorporation of Exfoliated Montmorillonite Nanoplatelets. *J. Polym. Sci., Part A: Polym. Chem.* **2008**, *46*, 47−53.

(7) Geng, Y.; Shi, Y.; Wang, L.; Ma, B.; Gao, R.; Zhu, Y.; Dong, H.; Qiu, Y. Photovoltage Improvements and Recombination Suppression by Montmorillonite Addition to PEO Gel Electrolyte for Dye-Sensitized Solar Cells. *Phys. Chem. Chem. Phys.* **2011**, *13*, 2417−2421.

(8) Lai, Y.-H.; Lin, C.-Y.; Chen, J.-G.; Wang, C.-C.; Huang, K.-C.; Liu, K.-Y.; Lin, K.-F.; Lin, J.-J.; Ho, K.-C. Enhancing the Performance of Dye-Sensitized Solar Cells by Incorporating Nanomica in Gel Electrolytes. *Sol. Energy Mater. Sol. Cells* **2010**, *94*, 668−674.

(9) Lee, C.-H.; Liu, K.-Y.; Chang, S.-H.; Lin, K.-J.; Lin, J.-J.; Ho, K.-C.; Lin, K.-Fu. Gelation of Ionic Liquid with Exfoliated Montmorillonite Nanoplatelets and its Application for Quasi-Solid-State Dye-Sensitized Solar Cells. *J. Colloid Interface Sci.* **2011**, *363*, 635−639.

(10) Chen, C. L.; Teng, H. S.; Lee, Y. L. In Situ Gelation of Electrolytes for Highly Efficient Gel-State Dye-Sensitized Solar Cells. *Adv. Mater.* **2011**, *23*, 4199−4204.

(11) Kwon, W.; Chang, Y. J.; Park, Y. C.; Jang, H. M.; Rhee, S. W. A Light Scattering Polymer Gel Electrolyte for High Performance Dye-Sensitized Solar Cells. *J. Mater. Chem.* **2012**, *22*, 6027−6031.

(12) Wu, C.; Jia, L.; Guo, S.; Han, S.; Chi, B.; Pu, J.; Jian, L. Open-Circuit Voltage Enhancement on the Basis of Polymer Gel Electrolyte for a Highly Stable Dye-Sensitized Solar Cell. *ACS Appl. Mater. Interfaces* **2013**, *5*, 7886−7892.

(13) Lee, H.-F.; Chua, Y.-T.; Yang, S.-M.; Hsu, P.-Y.; Ouyang, F.-Y.; Tung, Y.-L.; Kai, J. J. Efficient, Stable, and Flexible Dye-Sensitized Solar Cells based on Nanocomposite Gel Electrolytes. *Thin Solid Films* **2013**, *544*, 301−306.

(14) Dissanayake, M. A. K. L.; Divarathne, H. K. D. W. M. N. R.; Thotawatthage, C. A.; Dissanayake, C. B.; Senadeera, G. K. R.; Bandara, B. M. R. Dye-Sensitized Solar Cells Based on Electrospun Polyacrylonitrile (PAN) Nanofibre Membrane Gel Electrolyte. *Electrochim. Acta* **2014**, *130*, 76−81.

(15) Tao, L.; Huo, Z.; Dai, S.; Zhu, J.; Zhang, C.; Huang, Y.; Zhang, B.; Yao, J. Stable Quasi-Solid State Dye-Sensitized Solar Cell using a Diamide Derivative as Low Molecular Mass Organogelator. *J. Power Sources* **2014**, *262*, 444−450.

(16) Yuan, S.; Tang, Q.; Hu, B.; Ma, C.; Duan, J.; He, B. Efficient Quasi-Solid-State Dye-Sensitized Solar Cells from Graphene Incorporated Conducting Gel Electrolytes. *J. Mater. Chem. A* **2014**, *2*, 2814−2821.

(17) Neo, C. Y.; Gopalan, N. K.; Ouyang, J. Graphene Oxide/Multi-Walled Carbon Nanotube Nanocomposites as the Gelator of Gel Electrolytes for Quasi-Solid State Dye-Sensitized Solar Cells. *J. Mater. Chem. A* **2014**, *2*, 9226−9235.

(18) Yuan, S.; Tang, Q.; He, B.; Yang, P. Efficient Quasi-Solid-State Dye-Sensitized Solar Cells Employing Polyaniline and Polypyrrole Incorporated Microporous Conducting Gel Electrolytes. *J. Power Sources* **2014**, *254*, 98−105.

(19) Chen, H.-W.; Chiang, Y.-D.; Kung, C.-W.; Sakai, N.; Ikegami, M.; Yamauchi, Y.; Wu, K. C.-W.; Miyasaka, T.; Ho, K. C. Highly Efficient Plastic-based Quasi-Solid-State Dye-Sensitized Solar Cells with Light-Harvesting Mesoporous Silica Nanoparticles Gel-Electrolyte. *J. Power Sources* **2014**, *254*, 411−417.

(20) Yuan, S.; Tang, Q.; He, B.; Zhao, Y. Multifunctional Graphene Incorporated Conducting Gel Electrolytes in Enhancing Photovoltaic Performances of Quasi-Solid-State Dye-Sensitized Solar Cells. *J. Power Sources* **2014**, *260*, 225−232.

(21) Feng, Y.; Li, D.; Wang, Y.; Evans, D. G.; Duan, X. Synthesis and Characterization of a UV Absorbent-Intercalated Zn-Al Layered Double Hydroxide. *Polym. Degrad. Stab.* **2006**, *91*, 789−794.

(22) Guimaraes, J. L.; Marangoni, R.; Ramos, L. P.; Wypych, F. Covalent Grafting of Ethylene Glycol into the Zn−Al−CO_3 Layered Double Hydroxide. *J. Colloid Interface Sci.* **2000**, *227*, 445−451.

(23) Chang, Z.; Evans, D. G.; Duan, X.; Vial, C.; Ghanbaja, J.; Prevot, V.; de Roy, M.; Forano, C. Synthesis of [Zn−Al−CO_3] Layered Double Hydroxides by a Coprecipitation Method under Steady-State Conditions. *J. Solid State Chem.* **2005**, *178*, 2766−2777.
(24) Morel-Desrosiers, N.; Pisson, J.; Israeli, Y.; Taviot-Gueho, C.; Besse, J. P.; Morel, J. P. Intercalation of Dicarboxylate Anions into a Zn−Al−Cl Layered Double Hydroxide: Microcalorimetric Determination of the Enthalpies of Anion Exchange. *J. Mater. Chem.* **2003**, *13*, 2582−2585.
(25) Lombardo, G. M.; Pappalardo, G. C. Thermal Effects on Mixed Metal (Zn/Al) Layered Double Hydroxides: Direct Modeling of the X-Ray Powder Diffraction Line Shape through Molecular Dynamics Simulations. *Chem. Mater.* **2008**, *20*, 5585−5592.
(26) Bastianini, M.; Costenaro, D.; Bisio, C.; Marchese, L.; Costantino, U.; Vivani, R.; Nocchetti, M. On the Intercalation of the Iodine−Iodide Couple on Layered Double Hydroxides with Different Particle Sizes. *Inorg. Chem.* **2012**, *51*, 2560−2568.
(27) Islam, M.; Patel, R. Synthesis and Physicochemical Characterization of Zn/Al Chloride Layered Double Hydroxide and Evaluation of its Nitrate Removal Efficiency. *Desalination* **2010**, *256*, 120−128.
(28) Ding, P.; Qu, B. Synthesis and Characterization of Exfoliated Polystyrene/ZnAl Layered Double Hydroxide Nanocomposite via Emulsion Polymerization. *J. Colloid Interface Sci.* **2005**, *291*, 13−18.
(29) Wang, X.; Deng, R.; Kulkarni, S. A.; Wang, X. Y.; Pramana, S. S.; Wong, C. C.; Gratzel, M.; Uchida, S.; Mhaisalkar, S. G. Investigation of the Role of Anions in Hydrotalcite for Quasi-Solid State Dye-Sensitized Solar Cells Application. *J. Mater. Chem. A* **2013**, *1*, 4345−4351.
(30) Fabregat-Santiago, F.; Bisquert, J.; Garcia-Belmonte, G.; Boschloo, G.; Hagfeldt, A. Influence of Electrolyte in Transport and Recombination in Dye-Sensitized Solar Cells Studied by Impedance Spectroscopy. *Sol. Energy Mater. Sol. Cells* **2005**, *87*, 117−131.
(31) Huang, K. C.; Vittal, R.; Ho, K. C. Enhancing the Performance of Dye-Sensitized Solar Cells by Incorporating Nanomica in Gel Electrolytes. *Sol. Energy Mater. Sol. Cells* **2010**, *94*, 668−674.
(32) Jung, Y. S.; Yoo, B.; Lim, M. K.; Lee, S. Y.; Kim, K. J. Effect of Triton X-100 in Water-Added Electrolytes on the Performance of Dye-Sensitized Solar Cells. *Electrochim. Acta* **2009**, *54*, 6286−6291.
(33) Tai, S. Y.; Liu, C. J.; Chou, S. W.; Chien, F. S. S.; Lin, J. Y.; Lin, T. W. Few-Layer MoS_2 Nanosheets Coated onto Multi-Walled Carbon Nanotubes as a Low-Cost and Highly Electrocatalytic Counter Electrode for Dye-Sensitized Solar Cells. *J. Mater. Chem.* **2012**, *22*, 24753−24759.
(34) Boschloo, G.; Hagfeldt, A. Characteristics of the Iodide/Triiodide Redox Mediator in Dye-Sensitized Solar Cells. *Acc. Chem. Res.* **2009**, *42*, 1819−1826.